

## Chemical and TEM Studies of Chlorites in the Talc Deposits of the Chungnam Area, Korea

우리나라 충청남지역 활석광상에서 산출되는 녹니석의  
화학적 및 투과전자현미경 연구

Geon-Young Kim (김건영)\* · Soo Jin Kim (김수진)\*\*

\*Geoenvironmental Sciences Team, Korea Atomic Energy Research Institute, P.O. Box 105, Yusong, Taejeon 305-600, Korea  
(한국원자력연구소 심부지질환경특성연구분야, E-mail: kimgy@kaeri.re.kr)

\*\*Department of Geological Sciences, Seoul National University, Seoul 151-742, Korea  
(서울대학교 지질학과)

**ABSTRACT** : Chlorite from the talc deposits in the Chungnam area, Korea, has been studied using electron microprobe analysis and high resolution transmission electron microscopy (HRTEM). Talc ores are hydrothermal alteration products of serpentinite which was originated from ultramafic rocks. Chlorite occurs in close association with talc ores or with the black alteration zone between talc ore bodies and granitic gneiss. It is the most abundant impurity mineral of talc ores. Chlorite in association with talc is characterized by very high but narrow variations in Mg/(Mg+Fe) ratios (0.784~0.951), significant octahedral substitution (-0.200~0.692), wide variation in Al contents (1.085~3.160 / 14 oxygens), and high Cr and Ni contents. It was formed under a very limited but high Mg/(Mg+Fe) condition in close connection with serpentinite. Chlorite in the black alteration zone is characterized by a high Fe content, wide variation in Mg/(Mg+Fe) ratios (0.378~0.852), narrow octahedral substitution (-0.035~0.525), high narrow Al contents (1.468~2.959), and low Cr and Ni contents. It was formed under a low Mg/(Mg+Fe) and relatively Al-rich condition in close connection with country rocks. Two different chemical modes for chlorite suggest two different origins for two different chlorites. Although most of chlorites show typical 14-Å lattice fringe images under HRTEM, some chlorites show fringe images of 21-Å (14Å+7Å) spacings within (001) lattice-fringe images of chlorite (14Å). But brown chlorite from the black zone has high Ti and K contents suggesting that mica was the precursor of brown chlorite. Such possibility is also supported by the fact that lattice-fringe images of brown chlorite show 14-Å chlorite layers in which 10-Å mica single layer or packets are interlayered. Partial terminations from 3 mica layers to 2 chlorite layers are often observed. It, therefore, is suggested that the chlorite associated with talc ores is a hydrothermal alteration product of serpentinite, whereas the chlorites in the black alteration zone is a hydrothermal alteration product of granitic gneiss under a partial influence of serpentinite.

**Keywords** : chlorite, talc, high-resolution transmission electron microscopy (HRTEM), microstructure

요약 : 우리나라 충청남도 지역에 분포하는 활석광상에서 산출되는 녹니석에 대하여 전자현미분석 (EPMA) 및 고분해능투과전자현미경 (HRTEM)을 이용하여 연구하였다. 활석광석은 초염기성암기원 사문암의 열수변질산물이다. 녹니석은 활석광석을 구성하는 주요 불순광물이며, 산출상태에 따라 활석광석과 밀접한 관계를 갖고 산출되는 유형과 활석광체와 화강암질 편마암의 접촉부에 존재하는 검

은색의 변질대와 밀접한 관계를 갖고 산출되는 유형으로 나뉘어진다. 활석과 관련된 녹니석은  $Mg/(Mg+Fe)$ 비가 매우 높고, 좁은 변위를 보이며 (0.784~0.951), 상당한 팔면체 치환 (-0.0200~0.692) 및 넓은 범위의 Al 함량변화와, 높은 Cr과 Ni 함량으로 특징지어진다. 이 유형의 녹니석은 사문암과 밀접한 관계를 가지면서, 매우 제한되고 높은  $Mg/(Mg+Fe)$ 비를 갖는 환경에서 형성되었다. 검은색 변질대에서 산출되는 녹니석은 높은 Fe 함량 및 넓은 변위의  $Mg/(Mg+Fe)$ 비 (0.378~0.852)를 보이며, 좁은 범위의 팔면체 치환 (-0.035~0.525), 높고 좁은 Al 함량(1.468~2.959) 및 낮은 Cr과 Ni함량으로 특징지어진다. 이 유형의 녹니석은 주변암인 화강암질 편마암의 영향으로 낮은  $Mg/(Mg+Fe)$ 비를 갖고 상대적으로 Al이 풍부한 환경하에서 형성되었다. 이러한 녹니석에서 보여지는 두가지 유형의 화학적 특징은 두 유형의 녹니석이 두 가지 다른 생성 기원으로 생성되었음을 지시한다. 고분해능 전자현미경관찰에 의하면 비록 대부분 녹니석이 전형적인 14-Å의 격자이미지를 보이지만, 일부는 14-Å의 격자이미지 내에 21-Å(14Å+7Å)간격의 (001) 격자이미지를 보인다. 검은색 변질대에서 산출되는 갈색 녹니석은 높은 Ti 및 K 함량을 보여주는 것으로 보아 운모류의 변질산물로 여겨진다. 갈색 녹니석의 14-Å 격자이미지내에 운모류에 해당하는 10-Å의 단일 격자이미지 혹은 집합체가 관찰되는 사실이 이러한 설명을 뒷받침한다. 이밖에 HRTEM 관찰에서는 3개의 운모층에서 2개의 녹니석으로 전이되는 현상을 관찰할 수 있다. 따라서 활석광석과 관련된 녹니석은 사문암의 열수변질산물이며 반면에 검은색 변질대에서 산출되는 녹니석은 화강암질 편마암의 열수변질 산물로서 부분적으로 사문암의 영향을 받았다.

주요어 : 녹니석, 활석, 고분해능 투과전자현미경 (HRTEM), 미세구조

## Introduction

The Daeheung, Pyeongan, and Cheongdang (Shinyang) mines are three representative mines in the talc mineralized zone which trends north-northeast over the area of about 6 to 7 km in length and 10 to 100 m in width in the Chungnam area. There is little difference in mineralogy and occurrence of talc ores among three talc mines. A K-Ar dating of phlogopite coexisting with talc from the talc ore body yielded  $153 \pm 3$  M.Y., indicating that the formation of main talc ore body is late Jurassic, possibly in association with Daebo orogeny of Korea (Kim, 1997).

Talc ores of three representative talc mines in the area contain various impurity minerals such as chlorite, phlogopite, amphiboles, carbonates, and serpentine. They show thus very low values of whiteness. Among them chlorite is the major impurity mineral of talc ores. The talc mineralized zones are characterized by dark colored massive rock due to a high amount of chlorite (Kim and Kim, 1995). Abundant joints and small faults are observed in talc ore bodies and adjacent rocks. These joint and fault surfaces are typically coated with thin selvages of black mineral aggregates usually consisting

of chlorite and/or phlogopite. In addition, black-colored alteration zones are usually developed in contact zone between talc ore body and granitic gneiss.

The close association of chlorite with talc suggests that both have a close relation in their genesis. Although the possible origin of talc from chlorite schist or chlorite gneiss intercalated in the granitic gneiss has been suggested (Lee, 1994), talc and associated chlorite can be formed by hydrothermal steatitization of serpentinite, excluding minor amount of talc formed by alteration of chlorite at the late stage of steatitization.

Because phyllosilicate minerals from the area have similar habits, their textural and genetic relationships cannot be deciphered by ordinary petrographic method. Transmission electron microscopic method has been applied to this study, and genesis of chlorites has been studied on the chemical and microtextural viewpoints.

## Experimental Methods

X-ray powder diffraction (XRD) patterns of samples were obtained using a Rigaku Geigerflex with Ni-filtered CuK radiation. Polished thin sections were prepared and then carbon-

coated for electron microprobe analysis. Back-scattered electron (BSE) images were obtained with a JEOL JXA 733, fitted with a Link energy-dispersive X-ray (EDS) detector. Quantitative chemical analyses were performed using a wave dispersive X-ray spectrometer (WDS) controlled by a Link Specta System. Quantitative mineral analyses were done using standard ZAF correction procedures within the Specta software supplied by Link System. An operating voltage of 15 kV with a current of 10 nA was used for both the back-scattered imaging and the microprobe analysis. The beam diameter of 3~4  $\mu\text{m}$  was employed.

High-resolution transmission electron microscope (HRTEM) studies were performed to observe of microtextural relations and to obtain lattice fringe image for each sample using JEOL JEM-2000EXII transmission electron microscope which was operated at 200 kV accelerating voltage with a LaB<sub>6</sub> filament. Most of HRTEM images were recorded at a screen magnification of 250,000 $\times$ . In the present study, conventional double-tilting side-entry stage was used to obtain proper diffraction patterns for observation of the lattice-fringe images. Unfortunately, at the time of this TEM study, the resolution in many of the micrographs was degraded, and the brucite-like layers with chlorite were not fully resolved. However, it was still possible to recognize the positions of the brucite-like layers under these conditions by noting the anomalous spacings between the 2:1 layers and the lower contrast than that formed by typical chlorite structure where the brucite-like layers were not resolved.

### Occurrence of Chlorite

Chlorite is widely and abundantly found in the deposit as much as more than 70 percent in volume. It occurs in close association with talc either in the talc ore zone or in the black alteration zone between talc ore bodies and granitic gneiss. Chlorites from both zones show different occurrence and chemistry to each other. Chlorite from the talc ore zone and chl-

orite from the black alteration zone are referred to as the talc-related chlorite, and talc-unrelated chlorite, respectively.

In the talc deposits, chlorite aggregates occur surrounding large or small massive or irregular-shaped nodular talc ore bodies. The talc ore bodies themselves also contain variable amount of chlorite in a dispersed state. Thus the talc ores show grayish white to greenish gray tint. The contact of talc ores and the surrounding chlorite aggregates is gradational or sharp. In some case, it is observed that the nodular talc ores are surrounded by two or three thin layers of chlorite, brown phlogopite and/or acicular or fibrous tremolite. Tremolite occurring near the talc ore bodies is often altered to chlorite.

It is also observed under the optical and electron microscopes that chlorite is finely interleaved with phlogopite and/or talc (Fig. 1). Fine particles of chromite and Fe-Ni minerals are occasionally found in association with chlorite in talc ores. The 20~100  $\mu\text{m}$  thick coronas consisting of chlorite are found around chromite which in turn encloses brown chromian spinel.

Chlorite is also associated with the altered granitic gneiss, hornblende gneiss, dike rocks and quartz and pegmatite veins. Granitic gneiss in contact with talc ore bodies is highly altered to chlorite-biotite-albite rocks. Chlorite in dike rocks is an alteration product of mafic minerals of the rock. The dike rocks are not affected by steatitization. This type of chlorite is not directly associated with talc. Biotite, muscovite and amphibole are also found in the granitic gneiss, hornblende gneiss and dike rocks. Muscovite occurs only in the granitic gneiss.

In the black alteration zone with a thickness of 1~2 m, chlorite is usually fine-grained but occasionally coarse-grained. In addition to the typical chlorite, the chlorite showing brown interference color similar to biotite is found under the microscope (Fig. 2A) and it will be designated brown chlorite hereafter. It usually occurs as coarse-grained aggregates mainly in the black alteration zone between talc ore body and

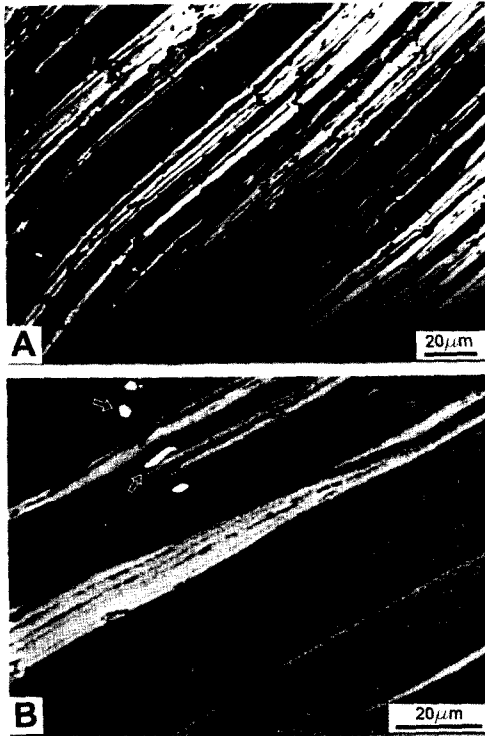


**Fig. 1.** A. BSE image of fine-scale interleavings of chlorite (dark) and phlogopite (light); B. BSE image plus X-ray image for Al showing the incoherent fine-scale intergrowths of talc (darker phase), phlogopite (light phase), and chlorite (white-dotted phase). The brightest phases arrowed are Fe-Ti minerals.

granitic gneiss. It has been identified as clinocllore of IIb polytype by XRD. It contains interleaved talc packets (Fig. 2A) and minute particles of Ti-bearing mineral (Fig. 2B). Scanning electron microscope (SEM) image of brown chlorite shows irregular-shaped flakes. BSE images of brown chlorite (Fig. 2B) show that Ti-minerals are dispersed within chlorite grain as coherently oriented packets or irregular forms.

Other minerals associated with talc ores are mica (phlogopite) and amphibole (tremolite-actinolite). Both minerals are of Mg-rich types in talc ores. Amphiboles show various habits such as acicular, fibrous and flaky under the microscope (Kim, 1997).

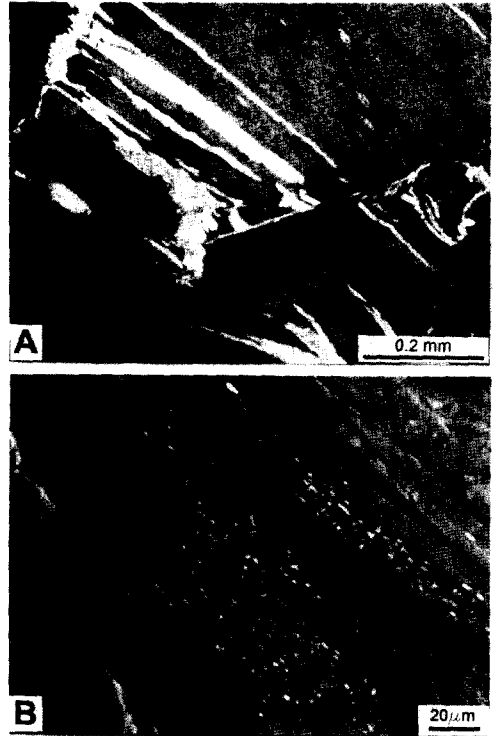


**Fig. 2.** A. Photomicrograph of brown chlorite. Talc packets (white) are interleaved in chlorite (grey); B. BSE image of brown chlorite. Ti-bearing minerals (white dots) are dispersed within chlorite grain as coherently oriented packets.

## Results

### *Chemistry of Chlorite*

Chemical analyses of representative chlorites of both types described above are given in Table 1. They have been normalized to 14 oxygens assuming that all irons are ferrous. Chlorites were classified following the classification scheme recommended by the Nomenclature Committee of AIPEA (Bailey, 1980). According to earlier work (Kim and Kim, 1995), the talc-related chlorites belong to clinocllore, whereas the talc-unrelated chlorites belong to clinocllore-chamosite. The talc-related chlorites show a moderate variation in Al content (1.085~3.160) and a very narrow variation in Fe/(Fe+Mg) ratios corresponding to

**Table 1.** Representative microprobe analyses of chlorite from the Chungnam area.

<sup>a</sup> Sample no.	E-23	R-3	R-16	Q-7	Q-11	C-37	E-10	P-2	R-10	R-12	Q-16	Q-18
<sup>b</sup> (N)	[2]	[3]	[3]	[3]	[3]	[4]	[5]	[4]	[4]	[3]	[3]	[4]
	talc-related chlorite						talc-unrelated chlorite					
SiO <sub>2</sub>	32.08	31.86	32.38	33.30	33.65	28.01	31.87	26.92	25.16	23.50	28.73	28.40
Al <sub>2</sub> O <sub>3</sub>	16.09	16.24	16.05	15.69	14.24	23.20	14.03	21.72	21.77	23.21	21.39	21.87
TiO <sub>2</sub>	0.07	0.03	0.01	0.24	0.10	0.00	0.00	0.04	0.07	0.09	0.06	0.06
Cr <sub>2</sub> O <sub>3</sub>	0.85	1.01	0.91	0.11	0.01	0.04	0.94	0.02	0.01	0.01	0.08	0.22
NiO	0.21	0.05	0.16	0.05	0.07	0.02	0.03	0.05	0.06	0.08	0.05	0.13
FeO	10.68	5.99	9.35	7.19	7.78	7.09	17.31	17.27	26.56	30.15	14.24	14.26
MgO	25.16	29.27	28.19	30.79	30.39	26.38	21.11	19.90	13.09	10.81	23.65	23.31
MnO	0.14	0.05	0.02	0.00	0.03	0.32	0.14	0.10	0.25	0.34	0.17	0.13
CaO	0.07	0.09	0.01	0.03	0.03	0.03	0.17	0.01	0.01	0.04	0.04	0.05
Na <sub>2</sub> O	0.01	0.02	0.02	0.00	0.00	0.03	0.02	0.02	0.02	0.01	0.01	0.02
K <sub>2</sub> O	0.72	0.00	0.55	0.32	0.18	0.00	0.00	0.22	0.08	0.04	0.00	0.00
Total	86.07	84.60	87.65	87.73	86.47	85.12	85.63	86.27	87.08	88.28	88.42	88.44
	cations per 14 oxygens											
Si	3.19	3.13	3.13	3.17	3.26	2.75	3.28	2.76	2.69	2.53	2.82	2.78
Al(IV)	0.81	0.87	0.87	0.83	0.74	1.25	0.72	1.24	1.31	1.47	1.18	1.22
Sum	4.00	4.00	4.00	4.00	4.00	4.00	4.00	4.00	4.00	4.00	4.00	4.00
Al(VI)	1.07	1.01	0.97	0.93	0.88	1.43	0.98	1.38	1.43	1.48	1.29	1.31
Ti	0.01	0.00	0.00	0.02	0.01	0.00	0.00	0.00	0.01	0.01	0.00	0.00
Cr	0.07	0.08	0.07	0.01	0.00	0.00	0.08	0.00	0.00	0.00	0.01	0.02
Ni	0.02	0.00	0.01	0.00	0.01	0.00	0.00	0.00	0.01	0.01	0.00	0.01
cFe	0.89	0.49	0.76	0.57	0.63	0.58	1.49	1.48	2.37	2.72	1.17	1.17
Mg	3.72	4.29	4.07	4.37	4.38	3.86	3.24	3.04	2.08	1.74	3.45	3.41
Mn	0.01	0.00	0.00	0.00	0.00	0.03	0.01	0.01	0.02	0.03	0.01	0.01
Ca	0.01	0.01	0.00	0.00	0.00	0.00	0.02	0.00	0.00	0.00	0.00	0.01
Na	0.00	0.00	0.00	0.00	0.00	0.00	0.00	0.00	0.00	0.00	0.00	0.00
K	0.09	0.00	0.07	0.04	0.02	0.00	0.00	0.03	0.01	0.01	0.00	0.00
Sum	5.88	5.89	5.95	5.95	5.93	5.91	5.83	5.95	5.94	5.99	5.94	5.94

<sup>a</sup>E-10, 23, P-2: Daeheung mine; R-3, 10, 12, 16: Pyeongan mine; Q-7, 11, 16, 18, C-37: Cheongdang mine

<sup>b</sup>Number of analyses

<sup>c</sup>All Fe calculated as Fe<sup>2+</sup>

clinochlore, whereas the talc-unrelated chlorites show a narrow variation in Al content (1.468 ~ 2.959) and a wide variation in Fe/(Fe+Mg) ratios from chamosite to clinochlore.

The talc-related chlorites show very high values and narrow variations in Mg/(Mg+Fe) ratios (0.784 ~ 0.951) with significant octahedral substitution of -0.200 ~ 0.692, whereas the talc-unrelated chlorites show wide variations in Mg/(Mg+Fe) ratios (0.378 ~ 0.852) with moderate

octahedral substitution of -0.035 ~ 0.525 (Fig. 8 in Kim and Kim, 1995). It is important that the Mg/(Mg+Fe) ratios of talc-related chlorites are different from those of talc-unrelated chlorites. The talc-related chlorites show less Tschermak substitutions, less Al contents, and more Mg and Si contents than the talc-unrelated chlorites. Cr and Ni contents are also higher in the talc-related chlorites than in the talc-unrelated chlorites.

**Table 2.** Microprobe analyses of brown chlorite from the Chungnam area.

<sup>a</sup> Sample No.	C-1	C-2	C-3	C-4	Average
SiO <sub>2</sub>	31.54	31.93	32.59	32.49	32.14
Al <sub>2</sub> O <sub>3</sub>	14.82	14.93	15.25	15.20	15.05
TiO <sub>2</sub>	0.94	1.44	0.65	0.46	0.87
Cr <sub>2</sub> O <sub>3</sub>	0.00	0.03	0.03	0.00	0.01
NiO	0.03	0.00	0.02	0.03	0.02
FeO	7.67	8.28	7.66	7.29	7.72
MgO	29.45	29.35	30.11	30.19	29.78
MnO	0.00	0.02	0.00	0.01	0.01
CaO	0.05	0.05	0.02	0.02	0.03
Na <sub>2</sub> O	0.00	0.00	0.01	0.02	0.01
K <sub>2</sub> O	0.33	0.26	0.35	0.35	0.32
Total	84.82	86.29	86.67	86.05	85.96
cations per 14 oxygens					
Si	3.13	3.12	3.15	3.16	3.14
Al(IV)	0.87	0.88	0.85	0.84	0.86
Sum	4.00	4.00	4.00	4.00	4.00
Al(VI)	0.86	0.84	0.89	0.90	0.87
Ti	0.07	0.11	0.05	0.03	0.06
Cr	0.00	0.00	0.00	0.00	0.00
Ni	0.00	0.00	0.00	0.00	0.00
<sup>b</sup> Fe	0.64	0.68	0.62	0.59	0.63
Mg	4.35	4.27	4.34	4.38	4.34
Mn	0.00	0.00	0.00	0.00	0.00
Ca	0.01	0.01	0.00	0.00	0.00
Na	0.00	0.00	0.00	0.00	0.00
K	0.04	0.03	0.04	0.04	0.04
Sum	5.96	5.93	5.95	5.96	5.95

<sup>a</sup>Sample from Cheongdang mine<sup>b</sup>All Fe calculated as Fe<sup>2+</sup>

Chemical analysis of brown chlorite from the black alteration zone (Table 2) show high Ti and K contents compared with the typical chlorite suggesting that mica is its precursor. Based on high Mg contents of brown chlorite, it is considered that the formation of brown chlorite might have been affected by serpentinite.

#### Transmission Electron Microscopic Study

Chlorite in Figs. 1 and 2 was observed under

the high resolution transmission electron microscope (HRTEM). HRTEM image indicates that most frequently observed chlorite is of 14-Å one-layer type (Fig. 3). However, it also shows deviating fringe images of 21-Å (14Å+7Å) spacings within (001) lattice-fringe images of 14Å. In addition, termination of chlorite layer is commonly observed (Fig. 3D). Electron diffraction pattern in the inset of Fig. 3A shows well-defined spots and weak streak (marked by arrow) probably resulting from the 21-Å layers, but does not show other regular odd-order reflections resulting from regularly mixed chlorite-7-Å layer. The 7-Å fringe is characterized by additional band within chlorite layers. This structure is due to the 1:1 structure of a single tetrahedral sheet and a single octahedral sheet in the chlorite structure. Bons and Scheyvers (1989) investigated four distinctive cases of chlorite using HRTEM and suggested that the local deviations of the (001) lattice spacing of 14-Å chlorite are caused by a local absence of the brucite interlayer resulting in a lattice spacing of 9Å or by layers with a 1:1 phyllosilicate structure of lattice spacing 7Å as seen in Fig. 3. Such deviating lattice-fringe spacings can be caused by variations in specimen thickness and orientation or electron-optical conditions. But, considering the electron diffraction pattern and ubiquitous occurrence of the deviating lattice-fringe spacings, they are certainly caused by actual variations in lattice-plane spacing, in which berthierine or other 7-Å phases are commonly regarded as a metastable precursor to chlorite in low grade metamorphic rocks or rocks undergoing diagenesis (Lee and Peacor, 1983; Veblen, 1983; Lee *et al.*, 1984; Ahn and Peacor, 1985; Amouric *et al.*, 1988).

The 21-Å spacings are mainly found in chlorite from the contact zone between talc ore body and serpentinite. Therefore, it is considered that the deviating fringe images of 21-Å (14Å+7Å) spacings within (001) lattice-fringe images of 14Å are metastable remnants of chlorite + serpentine reaction during steatiti-

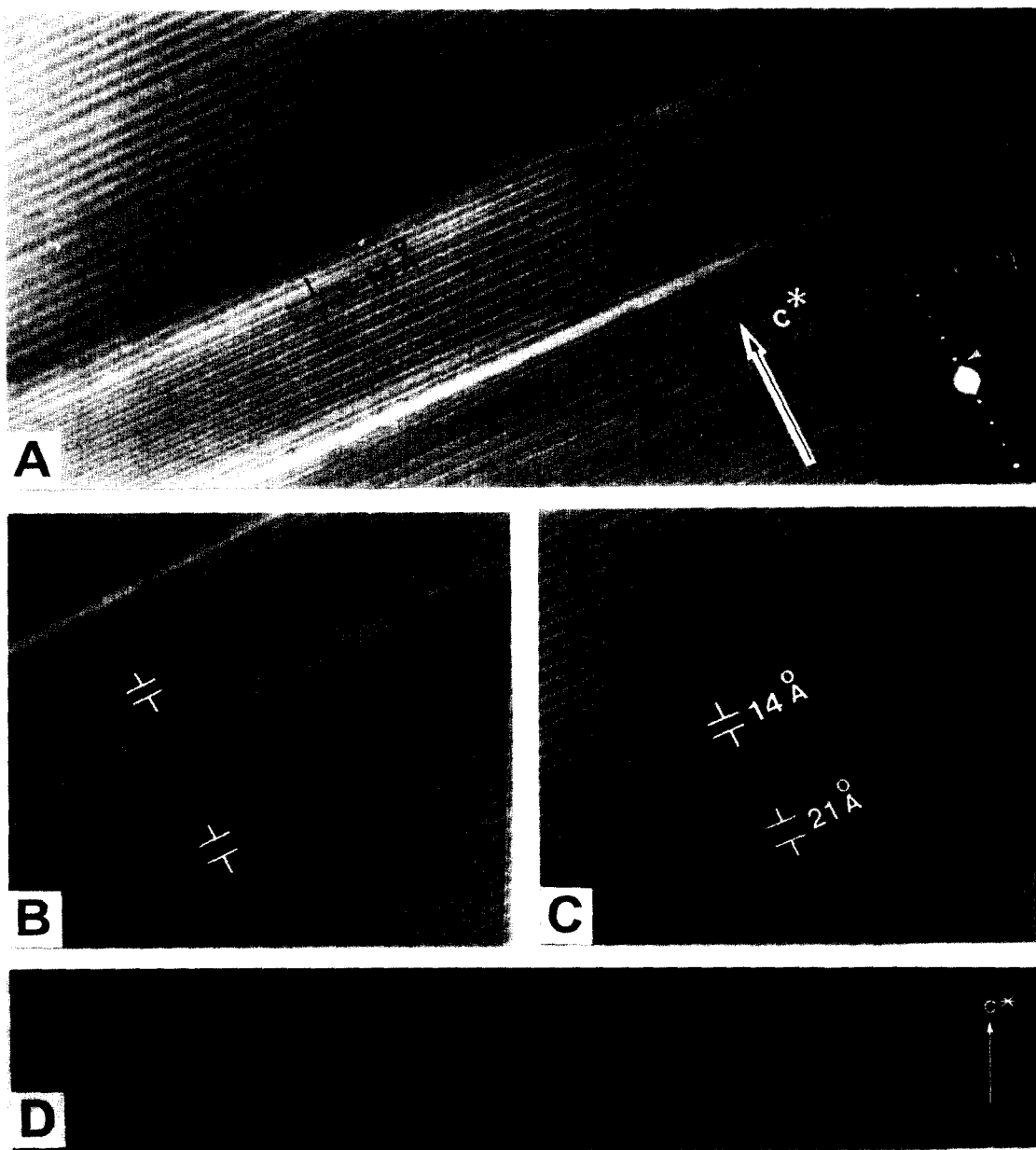


**Fig. 3.** Deviating fringe spacing in (001) lattice-fringe images of chlorites (sample P-16): A, B, and C. 21-Å (14Å+7Å) fringe within 14-Å fringes of chlorite. Diffraction pattern in A shows weak streak (marked by arrow) resulting from the 21-Å layers; D. Chlorite layer termination is common (marked by arrow).

zation of serpentinite. Chloritization as a common wall rock alteration of ultramafic rocks

is easily found at the margin of talc ore bodies. Many other interlayered HRTEM structures

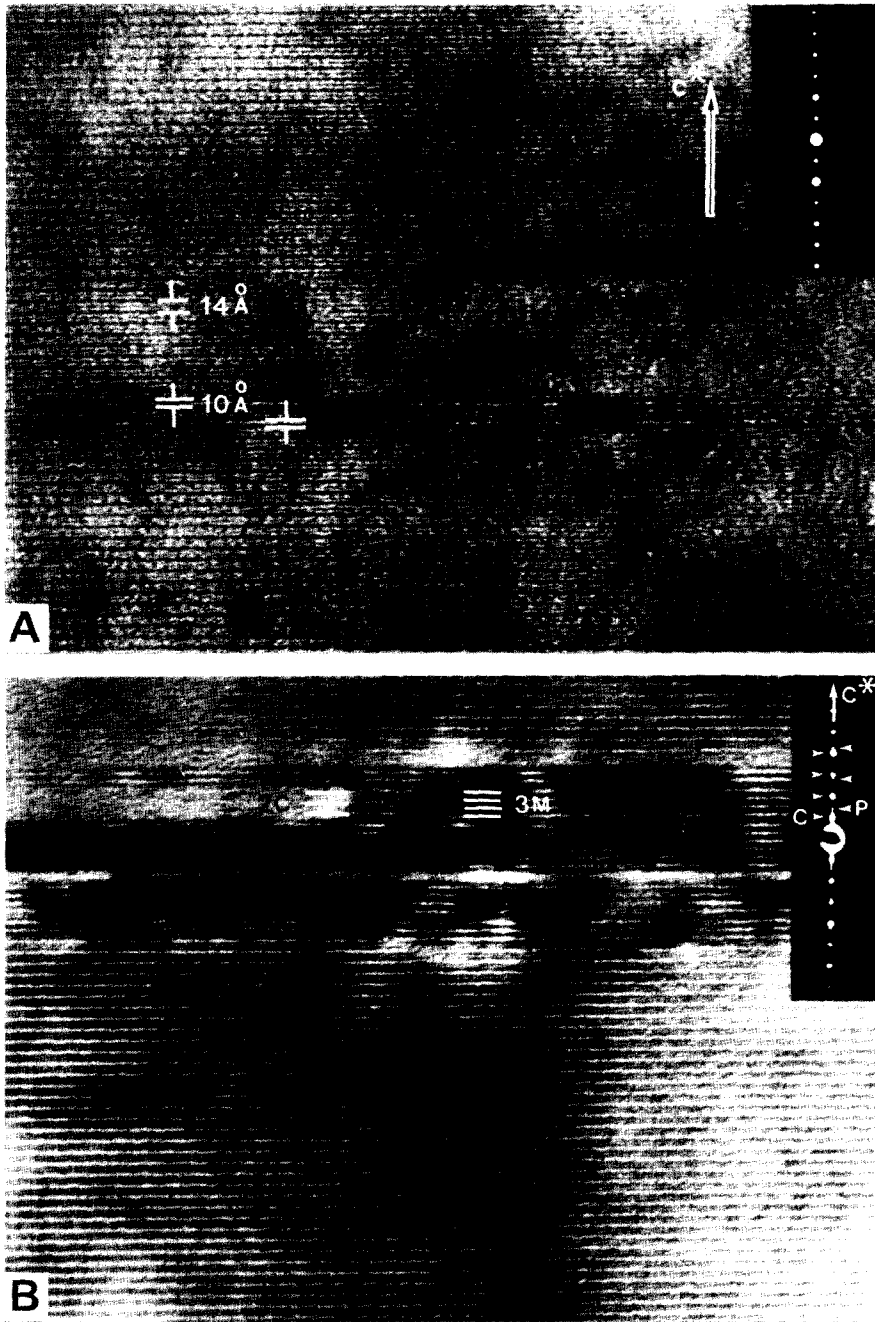


**Fig. 4.** Lattice fringe images and electron diffraction patterns: A. Brown chlorite showing single mica (10 Å) layers interlayered within chlorite (14 Å) layers; B. Brown chlorite consisting of chlorite ("C") layers and interleaved mica ("M") packets. Partial terminations from 3M to 2C are shown. Strain contrast, edge dislocations and bending of the nearby layers are found in association with the mica-chlorite layer terminations.



such as chlorite + mica and chlorite + talc can be easily found in this marginal zone of talc ores.

Lattice fringe image and electron diffraction pattern of brown chlorite show typical 14-Å chlorite layers (Fig. 4) in which mica (10 Å) layers are usually interlayered as single layer (Fig. 4A) or packets (Fig. 4B). In Fig. 4B, partial terminations from 3 mica layers to 2 chlorite layers are also shown. Especially, strain contrast, edge dislocations and bending of nearby layers are commonly found in association with mica-chlorite layer terminations.

### Discussion

Chlorite, due to its extensive solid solution, is a sensitive indicator of the extent of metasomatic alteration (Zhong *et al.*, 1985). Maruyama *et al.* (1986) suggested that the Fe/(Fe+Mg) ratios in chlorite from mafic rock can be used to monitor bulk rock Fe/(Fe+Mg) ratios. Zhong *et al.* (1985) proposed that the Fe/(Fe+Mg) and Al/(Al+Si) ratios of chlorite, as determined by electron microprobe analysis and X-ray diffractometry, seem to monitor the metasomatic exchange of Al, Fe and Mg between the metamorphosed ultramafic rocks and the country rock. Our earlier work (Kim and Kim, 1995) shows a good correlation in the MgO/(MgO+FeO) ratios between talc ores and associated chlorite. MgO/(MgO+FeO) ratios vary within a narrow range showing similar values to each other. In addition, the Mg/(Mg+Fe) ratios and the Al contents in octahedral or tetrahedral sites of chlorite are sensitive to whether they are related to talc in genesis or not. Chemical data also show that there are two distinct types of chlorites, that is, the talc-related chlorite and the talc-unrelated chlorite. Both types of chlorites have different occurrences and chemical compositions.

The field occurrences of talc and chlorite suggest that they have formed by hydrothermal alteration. The presence of two types of chlorites having different chemistry suggests two

different protoliths of different Mg/(Mg+Fe) ratios and Al contents, namely, serpentinite and granitic gneiss. The talc-related chlorite has very high but narrow variation in Mg/(Mg+Fe) ratios with significant octahedral substitution, wide variation in Al contents, and high Cr and Ni contents, suggesting that it was originated from serpentinite. It is assumed that this chlorite was formed under a limited high Mg/(Mg+Fe) conditions receiving various amounts of Al from granitic gneiss.

The talc-unrelated chlorite has high Fe content and wide variation in Mg/(Mg+Fe) ratios, narrow octahedral substitution, high and narrow Al values, and low Cr and Ni contents compared with the talc-related chlorite, suggesting that its composition might have been related to granitic gneiss surrounding the talc ore bodies. It was formed under a low Mg/(Mg+Fe) and relatively Al-rich conditions receiving various amount of Mg from serpentinite getting close to the composition of talc-related chlorite. The chemistry of the coexisting minerals such as mica and amphibole shows two different chemical behaviors similar to those of chlorite, supporting this interpretation.

The black alteration zone containing large amounts of chlorite is limited to the border zone. The chlorite in this zone is of Fe- and Al-rich type. The talc-related chlorites have a composition close to clinocllore, Mg end-member chlorite, with very narrow variation in Mg/(Mg+Fe) ratios. Therefore, the chemistry of chlorite suggests that the precursor of talc ores are not chlorite schist or chlorite gneiss but serpentinite originated from ultramafic rocks. Sanford (1982) shows that in northern Appalachian occurrences substitutions of Al for Si and Mg and Fe for Mg have diffused into the country rock and that this metasomatism is manifested in the chlorite composition. Al and Fe are distinctly abundant in chlorite, but Mg, Cr, and Ni are less abundant in chlorite of the country rock. These observations are consistent with data presented by Zhong *et al.* (1985) who showed increasing Al and Fe contents in chlo-

rite with increasing metasomatism of ultramafic rocks. Present study is in good accordance with their works.

Therefore, two different chemical behaviors of chlorite as well as coexisting minerals definitely indicate that the talc ore deposits have been formed by hydrothermal alteration of serpentinite originated from ultramafic rock and that the chlorites within the talc ores are not the remnants of steatitization of chlorite schist or chlorite gneiss, but the products formed mainly by metasomatic reaction of serpentinite with hydrothermal solution during steatitization. The chlorite aggregates within the altered gneiss at the border zone of talc ore bodies are not the relicts of steatitization of chlorite schist or chlorite gneiss but the reaction products of granitic gneiss with hydrothermal solution. The alteration history mentioned above is undoubtedly complex, involving retrogressive recrystallization from the original ultramafic assemblage plus chemical mass transfer between the granitic gneiss and the ultramafic intrusive. However, the chemistry and occurrences of chlorites were very useful to understand the general process of ore formation of the study area.

In addition to the chemistry of chlorite, microtextural study of chlorite gives some important information for the genetic interpretation of talc formation. The deviating fringe images of 21-Å (14Å+7Å) spacings within (001) lattice-fringe images of 14-Å chlorite (Fig. 3) as well as the 10-Å spacings interlayered within the chlorite (Fig. 4) indicate the interaction of serpentinite and granitic gneiss with hydrothermal solution. It is assumed that the chemistry of hydrothermal solution changed by its reaction with country granitic gneiss and serpentinite mainly at the border zone. During the hydrothermal alteration the metasomatic addition of Al<sub>2</sub>O<sub>3</sub> and K<sub>2</sub>O from hydrothermal solution to the parent rocks took place forming black alteration zone along the margins of the talc ore body. The constituent minerals of this zone are mainly chlorite and some mica. As mentioned above, their chemistry shows a tendency of spatial

dependence, showing Mg-rich compositions near talc ore body and serpentinite and Fe-rich compositions near granitic gneiss. During these processes of alteration, the hydrothermal solution often became partially more siliceous, thereby promoting steatitization, and where temporarily dammed, some pre-crystallized chlorites and/or micas altered to talc and/or chlorite during the late stage of steatitization. Therefore, during the early stage of steatitization of serpentinite, chlorite was formed from serpentine resulting in the deviating fringe images of 21-Å (14Å+7Å) spacings within the 14-Å chlorite. Because this process occurred in early stage, interlayering of 21-Å layers within the chlorite are rarely found.

In the late stage, some early crystallized micas altered to chlorite resulting in 10-Å layers interleaved within the 14-Å chlorite. This process is evidenced by the lattice HRTEM fringe images and partial terminations from 3 mica layers to 2 chlorite layers were observed. The reaction mechanism for this kind of transformation involves more than a simple addition or removal of K<sup>+</sup> and tetrahedral sheets of 2:1 layer. The mechanisms of such transformation between chlorite and mica were investigated by many mineralogists (Veblen and Ferry, 1983; Yau *et al.*, 1984; Eggleton and Banfield, 1985). One mechanism is the construction of brucite-like layers resulting in transformation from one mica layer to one chlorite layer and the other is a termination of talc-like layer resulting in transformation from two mica layers into a single chlorite layer. Both reactions are accompanied by a significant change in volume. However, the volume change can be compensated by combining both mechanisms of replacement resulting in a minimum of strain at the reaction front (Yau *et al.*, 1984). The possible structural relations for this transformation are shown in Fig. 4B. The lack of significant strain contrast associated with the interface in Fig. 4B also supports this explanation.

## Conclusions

The chlorites of the study area are classified into two types having different chemical behaviors, that is, the talc-related chlorite and the talc-unrelated chlorite. The talc-related chlorite is an alteration product of serpentinite which was originated from ultramafic rocks. Its chemistry is characterized by a very high and narrow variation in Mg/(Mg+Fe) ratios, significant octahedral substitution, wide variation in Al contents and high Cr and Ni contents. The talc-unrelated chlorite is an alteration product of granitic gneiss surrounding the talc ore bodies. Its chemistry is characterized by high Fe content and a wide variation in Mg/(Mg+Fe) ratios, high Al contents, and low Cr and Ni contents compared with the talc-related chlorite.

Microtextures of chlorite also give important information for their origin. Although most chlorites show typical 14-Å lattice fringe image under HRTEM, some chlorites show deviating fringe images of 21-Å (14Å+7Å) spacings within (001) lattice-fringe images of chlorites (14Å). Chlorite showing brown interference color shows high Ti and K contents suggesting that mica was the precursor of brown chlorite. Lattice fringe image and electron diffraction pattern of brown chlorite also show typical 14-Å chlorite layers within which mica (10Å) layers are interleaved as single layer or packets suggesting that mica was its precursor. Partial terminations from 3 mica layers to 2 chlorite layers were observed. All these microtextures suggest that the serpentinite and granitic gneiss reacted with hydrothermal solution to produce the mineral assemblages of the deposits. Therefore, the chemical behaviors as well as microtextures of chlorites and their coexisting minerals definitely indicate two different origins for the chemically different two chlorites and associated minerals.

## Acknowledgments

High resolution transmission electron mic-

roscope experiments were performed using the facility at the Inter-University Center for Natural Science Research, Seoul National University, and electron microprobe analyses were carried out at the Department of Geological Sciences, Seoul National University. This study was supported by the Project BSR1-97-5404 of the Ministry of Education, Korea.

## References

- Ahn, J. H. and Peacor, D. R. (1985) Transmission electron microscopic study of diagenetic chlorite in Gulf Coast argillaceous sediments. *Clays and Clay Minerals*, 33, 228-236.
- Amouric, M., Gianetto, I. and Proust, D. (1988) 7, 10 and 14 mixed-layer phyllosilicates studied structurally by TEM in pelitic rocks of the Piemontese zone (Venezuela). *Bulletin Mineralogique*, 111, 29-37.
- Bailey, S. W. (1980) Summary of the AIPEA nomenclature committee. *Can. Mineral.*, 18, 143-150.
- Bons, A.-J. and Schryvers, D. (1989) High-resolution electron microscopy of stacking irregularities in chlorites from the central Pyrenes. *Am. Mineral.*, 74, 1113-1123.
- Eggleton, R. A. and Banfield, J. F. (1985) The alteration of granitic biotite to chlorite. *Am. Mineral.*, 70, 902-910.
- Kim, G.-Y. and Kim, S. J. (1995) Chemistry of chlorite and its genetic significance in the talc deposits in the Yesan-Gongju-Cheounyang area. *J. Mineral. Soc. Korea*, 8, 91-107.
- Kim, G.-Y. (1997) Electron microscopic study on the talc mineralization in the Yesan-Gongju-Cheounyang area, Korea. Unpublished Ph.D thesis, Seoul National University, Korea, 259p.
- Lee, J. H. and Peacor, D. R. (1983) Intralayer transitions in phyllosilicates of Martinsburg shale. *Nature*, 303, 608-609.
- Lee, J. H., Peacor, D. R., Lewis, D. D. and Wintsch, R. P. (1984) Chlorite-illite/muscovite interlayered and interstratified crystals: A TEM/STEM study. *Contrib. Mineral. Petrol.*, 88, 372-385.
- Lee, S. H. (1994) Phase equilibria between coexisting minerals in the talc ores and process of talc formation in the Daehung Talc Deposits, Korea. *J. Petrol. Soc. Korea*, 3,

- 156-170. (in Korean)
- Maruyama, S., Cho, M. and Liou, J. G. (1986) Experimental investigations of blueschist-greenschist transition equilibria: pressure dependence of  $Al_2O_3$  contents in sodic amphiboles - A new geobarometer. In: Evans, B. W. and Brown, E. H. (Eds.) *Blueschists and eclogites*. Geol. Soc. Am. Memoir, vol. 164, 1-16.
- Sanford, R. F. (1982) Growth of ultramafic reaction zones in greenschist to amphibolite facies metamorphism. *Am. J. Sci.*, 282, 543-616.
- Veblen, D. R. (1983) Microstructures and mixed layering in intergrown wonesite, chlorite, talc, biotite and kaolinite. *Am. Mineral.*, 68, 566-580.
- Veblen, D. R. and Ferry, J. M. (1983) A TEM study of the biotite-chlorite reaction and comparison with petrologic observations. *Am. Mineral.*, 68, 1160-1168.
- Yau, Y.-C., Anovitz, L. M., Essene, E. J. and Peacor, D. R. (1984) Phlogopite-chlorite reaction mechanisms and physical conditions during retrograde reactions in the Marble Formation, Franklin, New Jersey. *Contrib. Mineral. Petrol.*, 88, 299-306.
- Zhong, W. J. S., Hughes, J. M. and Scotford, D. M. (1985) The response of chlorite to metasomatic alteration in Appalachian ultramafic rocks. *Can. Mineral.*, 23, 443-446.
- 
- 2000년 5월 6일 원고접수, 2000년 6월 7일 게재승인.